A paxillin tyrosine phosphorylation switch regulates the assembly and form of cell-matrix adhesions

Ronen Zaidel-Bar, Ron Milo, Zvi Kam and Benjamin Geiger*

Department of Molecular Cell Biology, Weizmann Institute of Science, Rehovot 76100, Israel

*Author for correspondence (e-mail: benny.geiger@weizmann.ac.il)

Accepted 16 October 2006
Journal of Cell Science 120, 137-148 Published by The Company of Biologists 2007
doi:10.1242/jcs.03314

Summary

Diverse cellular processes are carried out by distinct integrin-mediated adhesions. Cell spreading and migration are driven by focal complexes; robust adhesion to the extracellular matrix by focal adhesions; and matrix remodeling by fibrillar adhesions. The mechanism(s) regulating the spatio-temporal distribution and dynamics of the three types of adhesion are unknown. Here, we combine live-cell imaging, labeling with phosphospecific-antibodies and overexpression of a novel tyrosine phosphomimetic mutant of paxillin, to demonstrate that the modulation of tyrosine phosphorylation of paxillin regulates both the assembly and turnover of adhesion sites. Moreover, phosphorylated paxillin enhanced lamellipodial protrusions, whereas non-phosphorylated paxillin was essential for fibrillar adhesion formation and for fibronectin fibrillogenesis. We further show that focal adhesion kinase preferentially interacted with the tyrosine phosphomimetic paxillin and its recruitment is implicated in high turnover of focal complexes and translocation of focal adhesions. We created a mathematical model that recapitulates the salient features of the measured dynamics, and conclude that tyrosine phosphorylation of the adaptor protein paxillin functions as a major switch, regulating the adhesive phenotype of cells.

Supplementary material available online at
http://jcs.biologists.org/cgi/content/full/120/1/137/DC1

Key words: Paxillin, Tyrosine phosphorylation, Cell-matrix adhesion, Focal complexes, Focal adhesions, Fibrillar adhesions, Phosphomimetic, Fibronectin, Adhesion dynamics

Introduction

Integrin-mediated adhesions physically connect cells to the extracellular matrix (ECM), and serve as traction points, enabling cell spreading and migration (Kaverina et al., 2002). These sites also serve as signaling interfaces through which cells sense the chemical and physical properties of their environment (Geiger et al., 2001). The molecular machinery of integrin adhesions consists of a network of scaffolding and signaling proteins that link the integrin receptors to the actin cytoskeleton (Critchley, 2000; Zamir and Geiger, 2001). Cultured cells exhibit at least three types of integrin adhesions with distinct molecular composition, dynamics and function (Zamir and Geiger, 2001). Focal complexes (FXs) are dot-like adhesions that assemble under the lamellipodium in a hierarchical manner (Ballestrem et al., 2001; Kaverina et al., 2002; Nobes and Hall, 1995; Zaidel-Bar et al., 2003). Within less than a minute of their formation, FXs either turn over, or undergo a force-dependent transformation into focal adhesions (FAs) (Zaidel-Bar et al., 2003), which are considerably larger structures associated with actin- and myosin-containing stress fibers (Critchley, 2000; Geiger et al., 2001). Actomyosin contractility is required for the maintenance of FAs, as well as for their development into fibrillar adhesions (FBs) (Bershadsky et al., 2003; Wierzbicka-Patynowski and Schwarzbauer, 2003). The fibronectin (FN) receptor, $\alpha5\beta1$ integrin, and tensin are prominent components of FBs, which play an active role in FN fibrillogenesis (Pankov et al., 2000; Zamir et al., 2000).

Formation of these integrin adhesions is regulated by members of the Rho GTPase family. Specifically, Rac activity induces the formation of FXs, whereas activation of Rho leads to the induction and growth of FAs (Nobes and Hall, 1995; Rottner et al., 1999) and enhances FB formation (Wierzbicka-Patynowski and Schwarzbauer, 2003). However, the local molecular events that differentially regulate the properties of these adhesions and the transformation of one form into another are still poorly understood.

One of the mechanisms believed to be involved in FA assembly and turnover is tyrosine phosphorylation of FA proteins such as focal adhesion kinase (FAK), paxillin and p130cas (Panetti, 2002). These proteins undergo phosphorylation upon integrin engagement with the ECM (Bockholt and Burridge, 1993; Burridge et al., 1992); during spreading (Panetti, 2002); after serum stimulation (Barry and Critchley, 1994); or upon the formation of FAs (Burridge et al., 1992; Chrzanowska-Wodnicka and Burridge, 1994; Ridley and Hall, 1994). Moreover, inhibition of tyrosine phosphatase activity stimulates FAK and paxillin phosphorylation, and enhances focal adhesion assembly (Chrzanowska-Wodnicka and Burridge, 1994; Retta et al., 1996).

The main kinases believed to be responsible for tyrosine phosphorylation of FA molecules are $pp60^{c\text{-}src}$ (Src) and FAK (Frame, 2004; Schlaepfer and Mitra, 2004). Interestingly, FAK-null and Src-null cells, in which tyrosine phosphorylation of FA-associated proteins is reduced, display larger and more stable FAs than normal cells (Ilic et al., 1995; Volberg et al.,

2001). Moreover, the turnover of FAs is slower in the absence of FAK (Webb et al., 2004), and more rapid in cells lacking the tyrosine phosphatase Shp2 (von Wichert et al., 2003). However, the nature of the molecular targets of these phosphorylation events, and the mechanism(s) by which they regulate adhesion dynamics, are as yet unknown.

In the present study, we focus on the role of tyrosine phosphorylation of the FA-associated adaptor protein paxillin in the remodeling of integrin adhesions, and related cellular activities such as membrane protrusion and FN fibrillogenesis. Since the discovery of paxillin and the demonstration that it is a Src substrate (Glenney and Zokas, 1989) its central role as a scaffolding protein at the intersection of multiple adhesion-signaling pathways has been amply documented (Brown and Turner, 2004). Integrin activation, as well as growth factor stimulation, was shown to lead to the phosphorylation of paxillin on both tyrosine and serine residues (Bellis et al., 1997; Schaller and Schaefer, 2001). Serine phosphorylation was reported to have a role in FA targeting of paxillin (Brown et al., 1998), in cell spreading (Cai et al., 2006), and recently was implicated in regulating adhesion assembly via recruitment of a GIT-PIX-PAK complex (Nayal et al., 2006). Phosphorylation of two tyrosyl residues, namely Y31 and Y118, is induced upon integrin activation during epithelial-to-mesenchymal transition (Nakamura et al., 2000) and has been shown to enhance the migration of some cell types (Iwasaki et al., 2002; Petit et al., 2000), while inhibiting migration in others (Yano et al., 2000). The phosphorylation of Y31 and/or Y118 creates SH2 docking sites for Crk (Schaller and Parsons, 1995) or p120RasGAP (Tsubouchi et al., 2002), which are thought to be involved in the activation of Rac (Kiyokawa et al., 1998a; Kiyokawa et al., 1998b) or the inhibition of Rho (Tsubouchi et al., 2002). However, the significance of tyrosine phosphorylation of paxillin for adhesion dynamics and maturation remains unclear.

Here, we investigated the function of paxillin tyrosine phosphorylation by means of live-cell imaging and high-resolution, quantitative fluorescence microscopy. Our results demonstrate that tyrosine-phosphorylated paxillin is associated with FXs and FAs, but absent from FBs, and that the proportion of phosphorylated paxillin is negatively regulated by mechanical force. Overexpression of a phosphomimetic paxillin mutant enhances lamellipodial protrusion and formation of FXs and FAs, whereas cells overexpressing a non-phosphorylatable paxillin mutant display prominent FBs, and enhanced fibronectin fibrillogenesis. Interestingly, we found that FAK interacts preferentially with the phosphomimetic paxillin mutant and its overexpression triggers FA disassembly. Based on these results, as well as on previous data, we offer a comprehensive molecular and mathematical model, which addresses the cellular roles of the interplay between phosphorylated and non-phosphorylated paxillin, FAK recruitment, and the response to mechanical perturbation.

Results

Paxillin is differentially phosphorylated on Y31 and Y118 in different forms of integrin adhesions

As a first step in investigating the role of paxillin tyrosine phosphorylation in regulating cell adhesion, we double-immunolabeled porcine aortic endothelial cells (PAECs) with a general paxillin antibody, as well as with a phosphospecific antibody that recognizes paxillin, phosphorylated on residue Y118. Examination of the labeled cells indicated that the ratios between phosphopaxillin and paxillin are distinctly different in FXs, FAs and FBs (Fig. 1A). When compared with the intensity of total paxillin, we found that the proportion of Y118-phosphorylated paxillin in FXs was three times higher than in the nearby FAs. In FAs located around the cell center,

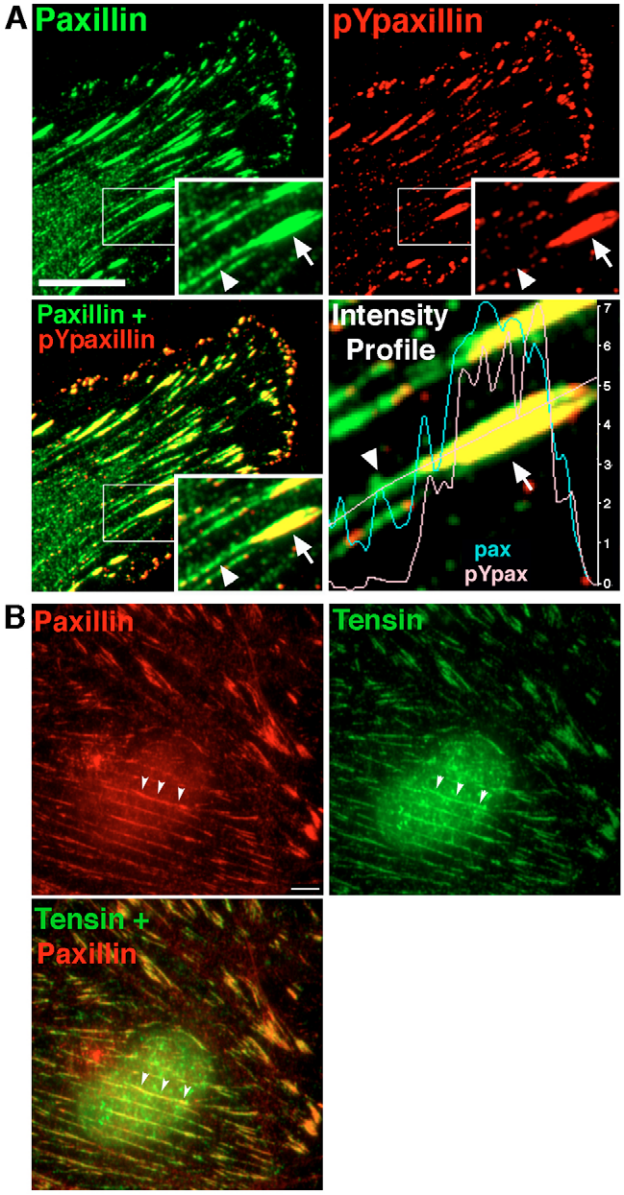

Fig. 1. Paxillin is tyrosine phosphorylated in focal complexes (FXs) and focal adhesions (FAs), but not in fibrillar adhesions (FBs). (A) Porcine aortic endothelial cells (PAECs) were fixed and double-stained for paxillin and phospho (Y118) paxillin. Arrows indicate an FA and arrowheads an FB. Note the high level of phosphorylated paxillin in FXs and FAs, and its absence in FBs. The intensity profile of paxillin (blue line) or phosphorylated paxillin (pink line) along a line one-pixel wide, spanning both an FA and an FB, is shown. (B) PAEC staining showing the co-localization of paxillin and tensin in both FA and FB. Bars, 10 μm (A); 5 μm (B).

paxillin Y118 phosphorylation was variable, and usually lower than that in peripheral FAs. Similar results were obtained with an antibody specific for Y31 phosphorylation.

Paxillin associated with FBs is not phosphorylated at either position Y31 or Y118 (subsequently, we used the Y118 antibody). Double-immunolabeling of paxillin and bona fide FB markers, tensin, or β_1 integrin, confirmed that non-phosphorylated paxillin is present, albeit at low levels, in FBs (Fig. 1B). This notion was corroborated by movies of YFP-paxillin, showing thin paxillin-containing fibrils extending from the inner tips of peripheral FA and transported centripetally (supplementary material Movie 1). The average intensity of paxillin along these FBs is about 30% of the intensity associated with large FAs. The border between phosphorylated paxillin in FAs, and non-phosphorylated paxillin in FBs emerging from the same FA, as well as the reduction in overall paxillin intensity, is sharp, as measured by intensity line profiles (Fig. 1A). The differential phosphorylation pattern of paxillin in FXs, FAs and FBs, described herein, was also reproduced in other cell types, such as rat embryo fibroblasts (REF52) (supplementary material Fig. S1).

Correlation between paxillin phosphorylation and reorganization of the adhesion site

To compare the dynamic properties of the three forms of integrin adhesion, we transfected PAECs with YFP-paxillin, and examined their adhesions by time-lapse video microscopy. Temporal ratio images, enabling comparison of the same cell at different time points, indicated that FBs are considerably more stable than FAs and FXs (Fig. 2A). We distinguished FBs from FAs by virtue of their lower intensity, thin and long morphology and central location in the cell. To quantify these differences, we used autocorrelation analysis. For that purpose, we segmented and defined specific FAs or FBs in the first frame of each movie; their area and intensity were then correlated with the fluorescence of the same pixels in each consecutive frame. An autocorrelation value of one indicates no change, and a value of zero indicates complete loss of the structure. The rate at which the correlation declines reflects the rate at which the adhesions disassemble, or diminish in intensity. Fig. 2B shows data for FAs and FBs, based on ten different movies (FXs were not included in this analysis, as their life spans were usually shorter than 1 minute). The

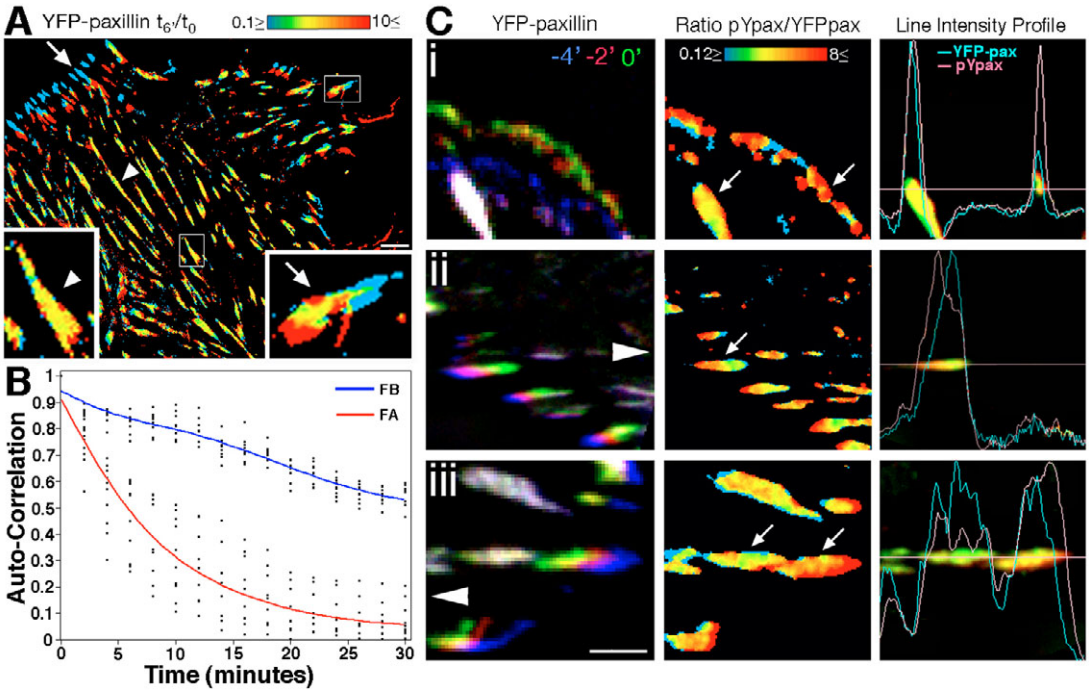

Fig. 2. Paxillin tyrosine phosphorylation is associated with both assembly and turnover of adhesions, whereas dephosphorylation correlates with adhesion stability. Time-lapse movies of cells expressing YFP-paxillin were analyzed by temporal ratio imaging (A) or by temporal autocorrelation analysis (B). At the end of the movie, cells were fixed and stained for phosphorylated paxillin, revealing the relationship between dynamics and phosphorylation state (C). Dividing intensity values of each pixel by the intensity in the same pixel 6 minutes earlier, created the temporal ratio image (A), which is presented in color, according to the look-up table. In general, red hues denote an increase in intensity or the appearance of new structures, blue hues denote structures that disappeared or decreased in intensity, and yellow marks unchanged pixels. Arrows indicate dynamic FAs, and arrowheads stable FBs. Inserts are enlarged four times. Similar movies were used to perform autocorrelation analysis for FBs and FAs separately (B). The area and intensity of chosen adhesions in the first frame of a movie were correlated with each consecutive frame. Data from ten movies is displayed, along with smoothing spline fits (λ=1000, FAs in red, FBs in blue). (C) Dynamics, presented by a three-color temporal overlay (left column); the phosphorylation status of paxillin, presented by a ratio image (middle column); and an intensity line profile of selected adhesions on a merged image (right column). Examples for three situations are presented: (i) assembly of FXs at the leading edge; (ii) disassembly in 'treadmilling' adhesions and (iii) a stable FA. Note that assembling FXs have the same intensity of phosphopaxillin as the focal adhesion, but only one-third of the intensity of paxillin (i). Note the shift in intensity profiles between paxillin and phosphopaxillin in the 'treadmilling' FA (right arrow) compared with a more stable adhesion (left arrow) (ii). Note the 30-40% decrease in phosphopaxillin intensity in the stable FA (iii). Arrowheads point to the cell center. Bars, 5 μm (A); 2 μm (C).

correlation decay time value corresponds to the time it takes the correlation to reach a value of 0.37 (1/e). The correlation decay time for FAs is 8.5 minutes, compared with 42 minutes for FBs (decay time of FX is <1 minute), implying that FX structures are considerably more dynamic than FAs, and both are more dynamic than FBs (Fig. 2B). It should be noted that we define adhesion 'dynamics' as a visible change in the area or location of the adhesion, and not as the rate at which molecules exchange between adhesion and cytosol.

Immunolabeling the cells expressing YFP-paxillin for phosphorylated paxillin at the end of the time-lapse movie enabled us to directly correlate the paxillin phosphorylation state with the recorded dynamic properties. Analysis of eight such movies led us to the following conclusions. (1) Newly formed adhesions always contain high levels of phosphorylated paxillin. This is best exemplified by FXs (Fig. 2Ci), but is also apparent in FAs located at the cell center. (2) In centripetally translocating FAs, which are probably 'treadmilling', phosphopaxillin levels in the disassembling 'tail' are always high, whereas paxillin in the assembling 'front' shows variable levels of phosphorylation (Fig. 2Cii). (3) FAs that remain stable in position and intensity usually contain low levels of phosphorylated paxillin (Fig. 2Ciii). (4) FBs do not contain phosphorylated paxillin from the instant they exit the focal adhesion. A similar analysis was performed with REF52 fibroblasts, stably expressing YFP-paxillin. Although the variations in phosphopaxillin levels in different integrin adhesions were not identical to those of PAECs, the trends described above were observed in these cells as well (supplementary material Fig. S1).

Expression of non-phosphorylatable or phosphomimetic mutants of paxillin affects the nature and dynamics of integrin adhesions

To test whether tyrosine phosphorylation merely affects the subcellular distribution of paxillin, or plays an active role in modulating integrin adhesion dynamics, we expressed different paxillin mutants in PAECs. For that purpose, we constructed two mutants of YFP-paxillin. In one, we replaced Y31 and Y118 with phenylalanine (Y2F), rendering the molecule non-phosphorylatable; in the second, we replaced the same residues with negatively charged glutamic acid (Y2E), which has been shown in other proteins to mimic constitutive tyrosine phosphorylation (Kassenbrock and Anderson, 2004; Potter et al., 2005; Tomar et al., 2004). The expression of exogenous paxillin resulted in a 30-50% increase in the level of paxillin in FAs, compared with non-transfected cells. The intensity of phosphopaxillin staining in cells expressing the mutants was less than half that in non-transfected cells, indicating that the majority of paxillin in these adhesions is exogenous (the phosphospecific antibody does not recognize the mutated Y2E paxillin, data not shown).

To our surprise, the expression of each mutant in PAECs dramatically affected the balance between adhesion forms. Manual counting of each adhesions type (n=3 cells) indicated that compared with wild-type cells Y2E had twice as many FXs and only one-tenth the number of FBs, whereas the number of FAs remained similar. Y2F cells, on the other hand, had half the number of FAs, one and a half times more FBs and one-tenth the number of FXs compared with wild-type cells (Fig. 3). Immunolabeling of the transfected cells for tensin (an FB marker) and phosphotyrosine (an FX and FA marker) confirmed that the change in adhesive phenotype is genuine, and is not merely due to selective localization of the mutant proteins (Fig. 3). Similar effects of the Y2E and Y2F constructs were also observed in NIH3T3 fibroblasts, confirming that the phenomenon is rather general (supplementary material Fig. S2). Since the Y2E-paxillin induces an adhesive phenotype identical to the localization of phosphorylated paxillin we refer to this mutant as 'phosphomimetic'.

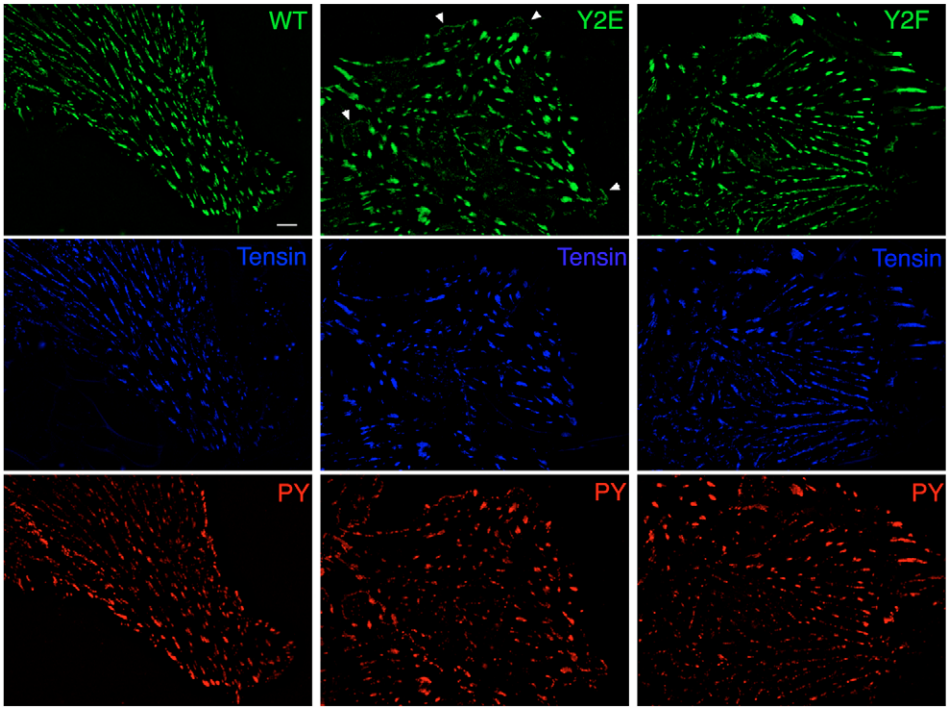

Fig. 3. Phosphomimetic and non-phosphorylatable paxillin mutants affect the adhesive phenotype of endothelial cells. Porcine aortic endothelial cells were transfected with phosphomimetic (Y2E) or non-phosphorylatable (Y2F) mutants of YFP-paxillin and with wild-type YFP-paxillin as a control. To verify that the lack of FB in Y2E cells and the lack of FX in Y2F cells was genuine, the transfected cells were stained for tensin (blue) and general phosphotyrosine (PY, red). Bar, 5 μm.

To characterize the effects of constitutive paxillin phosphorylation or dephosphorylation on the assembly and disassembly rates of integrin adhesions, we compared the adhesion dynamics of cells expressing the two mutants with that of cells expressing wild-type paxillin. We show that in the Y2E-paxillin-expressing cells, FXs and FAs assemble and disassemble at an increased rate, reflected in the abundance of red and blue pixels in the temporal ratio images. Y2F-paxillin-expressing cells, on the other hand, form much more stable adhesions, dominated by yellow pixels (Fig. 4A; supplementary material Movie 2).

To quantify the change in adhesion dynamics induced by the mutants, we performed autocorrelation analyses on seven movies of each mutant and wild-type paxillin (Fig. 4B, 'whole cell'). The mean correlation decay time for wild-type paxillin was 28 minutes; for Y2E-paxillin, it was 19 minutes; and for Y2F-paxillin, it increased up to 45 minutes. Evidently, these are average values of paxillin dynamics in FBs, FAs and FXs, which greatly differ. Therefore, the altered dynamics of the mutants could simply reflect the altered balance between FAs, FXs and FBs. To directly examine this possibility, we compared, by autocorrelation analysis, the dynamics of Y2E-paxillin to wild-type FAs, and Y2F-paxillin to wild-type FBs (Fig. 4B, 'FA/FB specific'). These analyses showed that the wild-type paxillins in FB and Y2F-paxillin were similarly stable. By contrast, Y2E-paxillin was 25% more dynamic than wild-type paxillin in FA.

FN fibrillogenesis, actin organization and lamellipodial activity depend on the phosphorylation state of paxillin

The absence of FB from cells expressing Y2E-paxillin and their enrichment in cells expressing Y2F-paxillin, raised the possibility that the phosphorylation status of paxillin might also affect actin organization and FN fibrillogenesis. To address this issue, we labeled cells expressing the two paxillin mutants for either actin or FN. Non-transfected PAECs, as well as cells overexpressing wild-type paxillin, displayed parallel arrays of stress fibers spanning the entire cell (Fig. 5A). Cells expressing Y2E-paxillin retained the ability to form stress fibers. However, in the majority of the cells, actin bundles were relatively short, and restricted to the cell periphery. Cells expressing Y2F-paxillin, on the one hand, displayed enhanced assembly of long stress fibers (Fig. 5A), and dramatically augmented FN fibrillogenesis. Expression of Y2E-paxillin, on the other hand, suppressed this process (Fig. 5B), suggesting that paxillin dephosphorylation is essential. Quantification of the extent of fibronectin fibrillogenesis by measuring the average intensity of fibronectin staining per cell is shown in Fig. 5C.

Our observation that Y2E-paxillin expression enhanced FX formation, whereas FXs were absent in Y2F-paxillin-expressing cells, raised the possibility that phosphorylated paxillin enhances lamellipodial activity, which, in turn, stimulates FX formation. To test this possibility, we directly counted the frequency of lamellipodial extensions by PAECs expressing the wt or mutant paxillins. Based on five 2-hour movies, we found that cells expressing wild-type-paxillin produce an average of 4.4±1.7 protrusions/hour. Cells expressing Y2E-paxillin produced 25% more protrusions (5.5±0.8), whereas the protrusive activity of Y2F-paxillin expressing cells was severely suppressed (1.8±2.4 protrusions/hour).

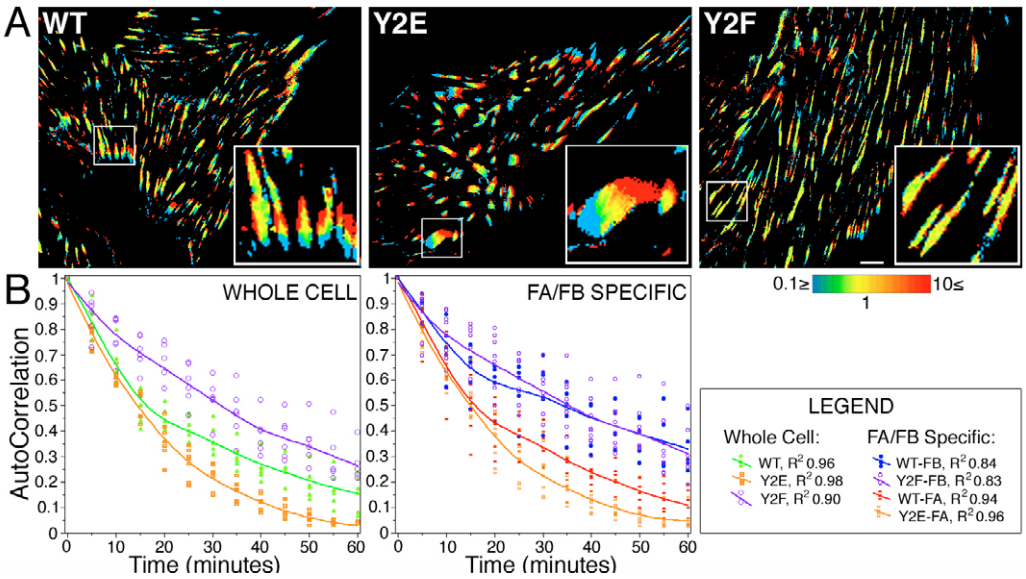

Fig. 4. Phosphomimetic paxillin enhances adhesion dynamics and non-phosphorylatable paxillin stabilizes adhesion sites. Time-lapse movies of endothelial cells, expressing wild-type YFP-paxillin or phosphomimetic (Y2E) or non-phosphorylatable (Y2F) mutants, were used to create temporal ratio images (A) and for autocorrelation analysis (B). For each construct, the ratio between two time points, 10 minutes apart, is presented in color code, such that new pixels are red, pixels that disappeared are blue and unchanged pixels are yellow. Note the high proportion of red and blue pixels in Y2E-paxillin and the predominance of yellow pixels in Y2F-paxillin. Inserts are enlarged three times. For each construct, seven movies were used to perform autocorrelation analysis, either on the whole cell or specifically for FA/FB. Autocorrelation is calculated by comparing the adhesions in each time point with time zero. All points are plotted, as well as smoothing spline fits (λ=1000) as specified to the right. Bar, 5 μm.

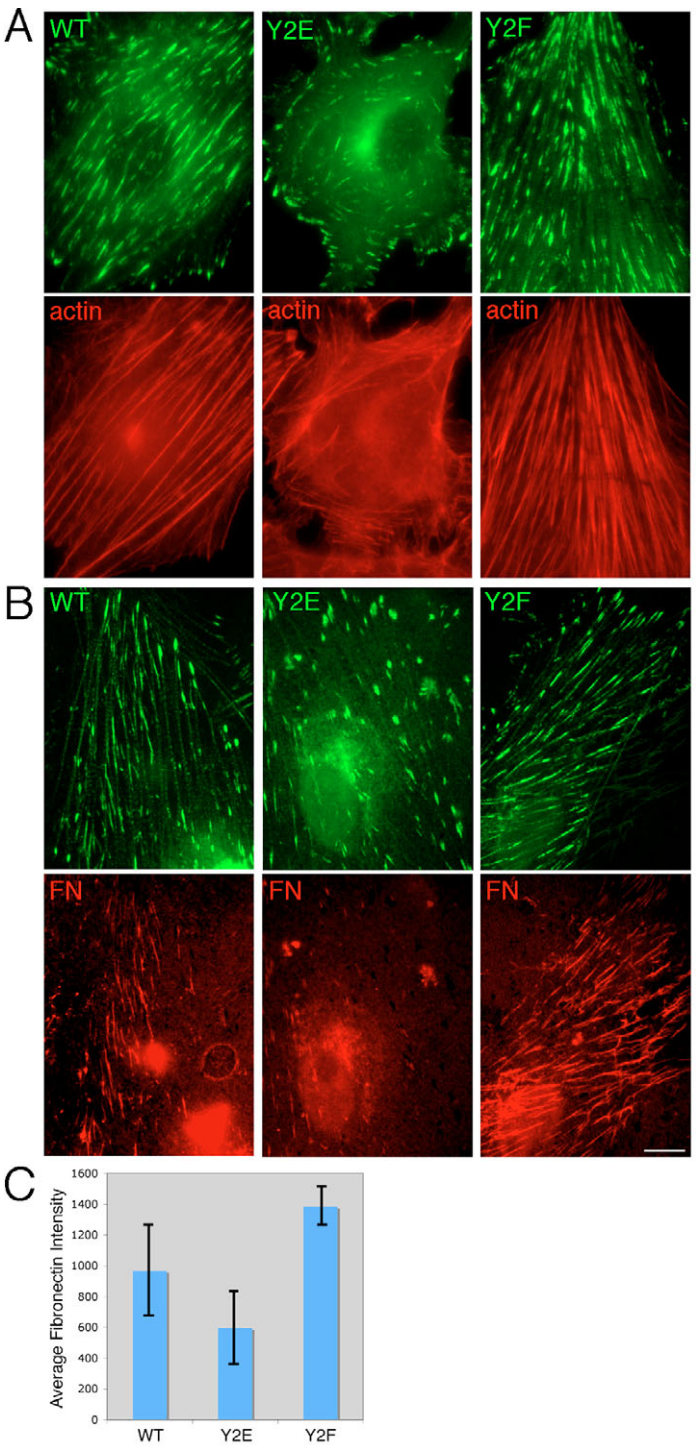

Fig. 5. Phosphomimetic paxillin inhibits the formation of long stress fibers and fibronectin fibrillogenesis. Cells expressing wild-type or mutant YFP-paxillin were grown for 48 hours and then fixed and stained for F-actin (A) and fibronectin (B). In cells expressing the phosphomimetic mutant (Y2E) there is a conspicuous absence of long actin stress fibers, whereas they are overly abundant in the non-phosphorylatable mutant (Y2F) (A). Similarly, fibronectin fibrillogenesis is impaired in Y2E, and enhanced in Y2F (B). (C) The extent of fibronectin fibrillogenesis was quantified by measuring the average intensity of fibronectin per cell (n=10). Means ± s.d. are shown. Bar, 5 μm.

Paxillin phosphorylation is regulated by mechanical force

As shown above, the transition from FX to more stable FA is accompanied by a reduction in local phosphopaxillin-to-paxillin ratio. We have previously demonstrated that the FX-FA transition is force dependent (Zaidel-Bar et al., 2003). In line with this, we have recently shown that under shear flow conditions the relative levels of phosphopaxillin decline, whereas force reduction elevates phosphopaxillin levels (Zaidel-Bar et al., 2005). Here we provide further support for this idea by using a pharmacological inhibitor of actomyosin contractility (H7). As expected, inhibition of actomyosin contractility caused the dissolution of FA within 10 minutes. However, 1 minute after application of the drug, the intensity of paxillin remained similar to that of untreated controls, whereas there was a dramatic increase in phosphopaxillin levels (Fig. 6). Similar results were attained using blebbistatin as an inhibitor of myosin and Y27832 as an inhibitor of ROCK (data not shown).

Phosphorylated paxillin recruits FAK, leading to increased adhesion turnover

The marked difference between phosphorylated and non-phosphorylated paxillin (represented by the respective mutants) in their effect on cell adhesion raised the possibility that they differ in their interaction with specific target proteins. The fact that our novel tyrosine phosphomimetic and non-phosphorylatable mutants had varying effects on integrin adhesion offered an opportunity to examine the binding properties of the two molecules biochemically. Purified glutathione S-transferase (GST)-tagged fusion proteins of wild-type paxillin and of the two mutants were used to pull down interacting protein(s) from PAEC cell extracts. Western blot analysis of these complexes, using phosphotyrosine antibodies, revealed several bands that were substantially stronger in the Y2E lane, and weaker in the Y2F lane, compared with wild-type paxillin. We identified one band at ~70 kDa as paxillin, and another band at ~115 kDa as FAK (Fig. 7A). Additional bands at ~50 kDa and ~55 kDa remain unidentified (data not shown). Based on four separate pull-down assays it was found that the Y2E mutant was capable of pulling down about 2.5 times more FAK than wild-type paxillin, whereas the Y2F mutant pulled down less than half that of the wild-type paxillin (Fig. 7B). These results suggest that it is predominantly the phosphorylated form of paxillin that interacts with FAK and recruits it into the adhesion sites.

To substantiate this hypothesis in living cells, we stained PAECs expressing either Y2E or Y2F paxillin with a phosphospecific antibody reacting with activated FAK (phosphorylated at the autophosphorylation site on Y397). Indeed, Y2E-paxillin expression induced the recruitment of higher levels of active FAK to FAs, compared with non-transfected neighboring cells. The Y2F-paxillin mutant, on the other hand, dramatically suppressed the accumulation of endogenous FAK in the adhesion sites (Fig. 7C). We quantified the intensity of FAK (Y397) in association with adhesions containing mutant paxillin in eight different cells, and compared the intensity with that measured in eight non-transfected cells. The results (Fig. 7D) show that FAK recruitment was strongly suppressed (~90%) by the

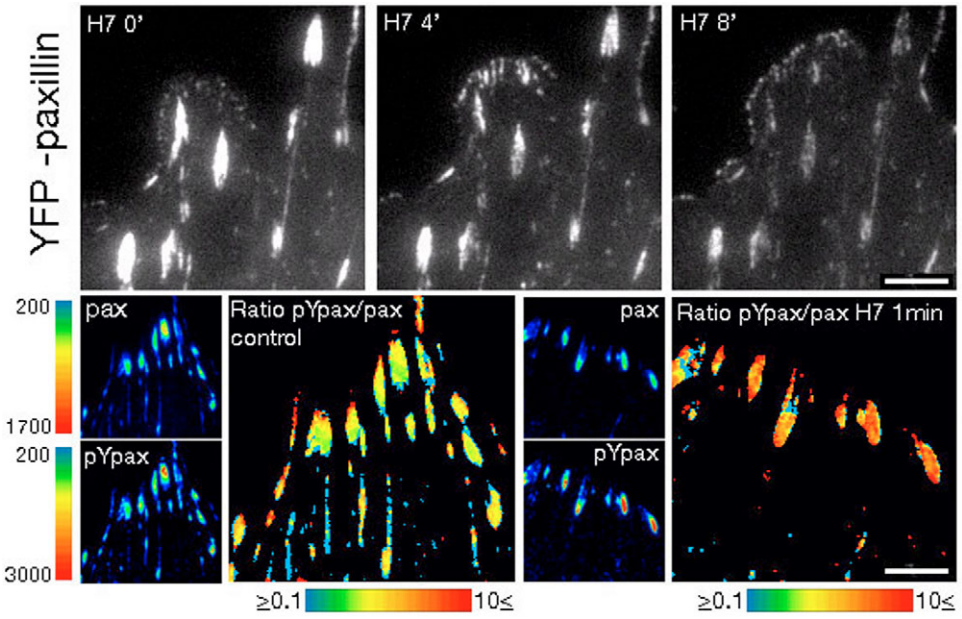

Fig. 6. Paxillin phosphorylation is regulated by mechanical force. Treatment with an actomyosin contractility inhibitor (H7) leads to disassembly of FAs and formation of FXs, as seen in the frames from a time-lapse movie of PAECs expressing YFP-paxillin (top). Preceding the disassembly there is an increase in paxillin phosphorylation levels, as indicated by immunolabeling of cells for paxillin and phosphopaxillin after 1 minute of treatment with H7 (bottom). Single labels are spectrum scaled for intensity, using the same scale for control and treated cells. The ratio image was scaled according to the provided look-up table. Bar, 5 μm.

Y2F mutant. Expression of Y2E-paxillin, on the other hand, enhanced FAK (Y^{397}) recruitment by ~25% (P<0.05). Further support for the idea that phosphorylated paxillin is responsible for recruiting FAK into adhesions was found in double immunostainings of PAECs for FAK and phosphopaxillin, or FAK and tensin. These experiments show perfect co-localization of FAK with phosphopaxillin; moreover, FAK is poorly co-localized with tensin in FB, where paxillin is not phosphorylated (supplementary material Fig. S3).

FAK could positively regulate FA turnover (Hamadi et al., 2005; von Wichert et al., 2003; Webb et al., 2004), raising the possibility that Y2E-paxillin increases FA dynamics through its ability to recruit FAK. To test whether the increased FA dynamics induced by Y2E-paxillin is indeed FAK-dependent or acts through a separate pathway, we transfected the paxillin

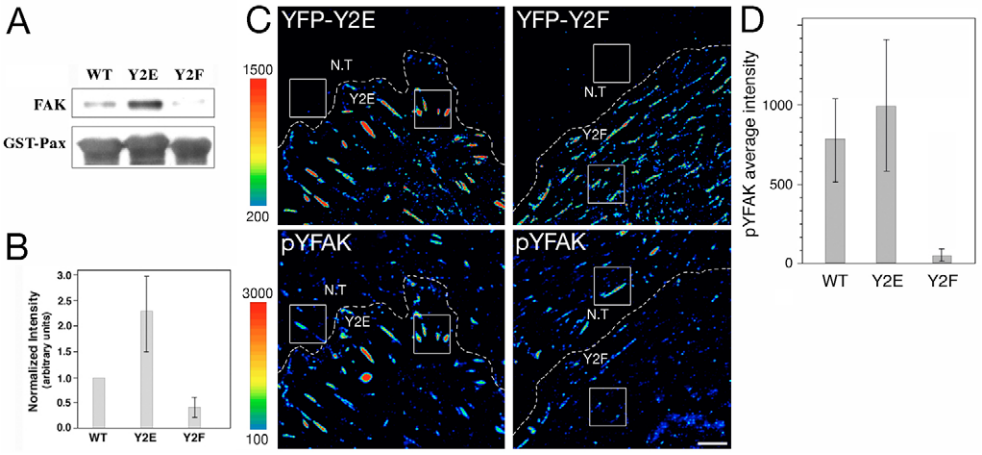

Fig. 7. FAK interacts preferentially with tyrosine phosphorylated paxillin in vitro and in vivo. Purified GST-fusion proteins of wild-type, phosphomimetic (Y2E) or non-phosphorylatable (Y2F) paxillin were used to pull down proteins from equal amounts of endothelial cell extract, followed by western blotting for FAK. A representative blot is shown (A) as well as quantification of the mean (± s.e.) of four separate pull-down experiments (B). Localization of phosphorylated FAK (Y397) was examined by staining in PAECs expressing mutant paxillin alongside non-transfected (N.T) neighboring cells. Images in C are colored according to an intensity scale, as indicated. For convenience of comparison, squares mark adhesions in transfected and non-transfected neighboring cells. (D) Eight transfected or non-transfected cells were segmented and the intensity of pYFAK (means ± s.d.) in each adhesion was calculated. Bar, 5 μm.

mutants into FAK-null fibroblasts, as well as FAK-null cells re-expressing FAK. Autocorrelation analyses performed on time-lapse movies of these cells revealed that although FA dynamics in FAK-null cells are somewhat slower than in FAK re-expressing cells, they are not affected by the expression of either paxillin mutant (Fig. 8A). In the FAK re-expressing cells, paxillin mutants display differential dynamics, confirming that the effect of phosphopaxillin on adhesion dynamics is indeed mediated by FAK. In line with these results, we found that overexpression of FAK in PAECs leads to a doubling of FA turnover, as measured by autocorrelation analysis. There is no further effect on adhesion dynamics when Y2E-paxillin or Y2F-paxillin mutants are co-transfected with FAK (Fig. 8B and supplementary material Movie 3), indicating that recruitment by phosphopaxillin becomes irrelevant under conditions of FAK overexpression.

Discussion

In this study we have demonstrated the central role of tyrosine phosphorylation of paxillin in the regulation of the assembly and turnover of different forms of integrin adhesions. This conclusion is based on several lines of evidence: paxillin phosphorylation (on tyrosine residues 31 and 118) is very prominent in FX. A tyrosine phosphomimetic paxillin mutant, used here for the first time, dramatically enhances FX formation. Moreover, the expression of another mutant paxillin, lacking the two phosphorylation sites, suppresses FX formation. These discoveries indicate that paxillin phosphorylation is essential for the assembly of FX and, possibly, for the stimulation of lamellipodial protrusions. Notably, both structures are induced by the activation of Rac, which could be stimulated by phosphopaxillin through its effect on the CrkII-DOCK180 pathway (Kiyokawa et al., 1998a; Kiyokawa et al., 1998b) or via inhibition of Rho through the binding of p120RasGAP (Tsubouchi et al., 2002). It should be noted that phosphorylation of these sites was previously suggested to be important for the formation of FA (Turner et al., 1995) and for cell spreading (Richardson et al., 1997) and migration (Iwasaki et al., 2002; Nakamura et al., 2000; Petit et al., 2000) on the basis of experiments using a non-phosphorylatable mutant of paxillin.

Our work indicates that paxillin phosphorylation affects integrin adhesions as a double-edged sword: it stimulates the assembly of FX, yet it also induces adhesion turnover (probably, through the recruitment of FAK, see below). This was initially suggested by the close correlation between endogenous paxillin phosphorylation levels and the turnover of the corresponding adhesion sites, and corroborated by the dramatic opposite effects of the phosphomimetic and non-phosphorylatable paxillin mutants on FA turnover.

Adhesions containing different proportions of phosphorylated and non-phosphorylated paxillin display marked differences in dynamics. Results presented here, as well as previous work from our lab, strongly suggest that the switch in paxillin-phosphopaxillin ratio is regulated by mechanical force. This was demonstrated by the application of physiological levels of shear stress (Zaidel-Bar et al., 2005) and by inhibition of contractility. While the relative amount of phosphopaxillin is negatively regulated by force, our data cannot determine whether force induces the selective recruitment of non-phosphorylated paxillin, or induces dephosphorylation of phosphopaxillin. In the case of dephosphorylation in response to force, one cannot exclude effects via inhibition of a kinase or activation of a phosphatase.

Our novel findings suggest that the increase in adhesion disassembly induced by phosphopaxillin is directly caused by the recruitment of FAK. This is evident from the inability of Y2E paxillin to increase adhesion turnover in FAK-null cells, and is corroborated by the capacity of overexpressed FAK to facilitate FA turnover, even in the presence of excess Y2F paxillin. It is well established that FAK is recruited to FAs through its binding to the second and fourth LD domains of paxillin, which span residues 143-164 and 265-313, respectively (Hayashi et al., 2002; Tachibana et al., 1995).

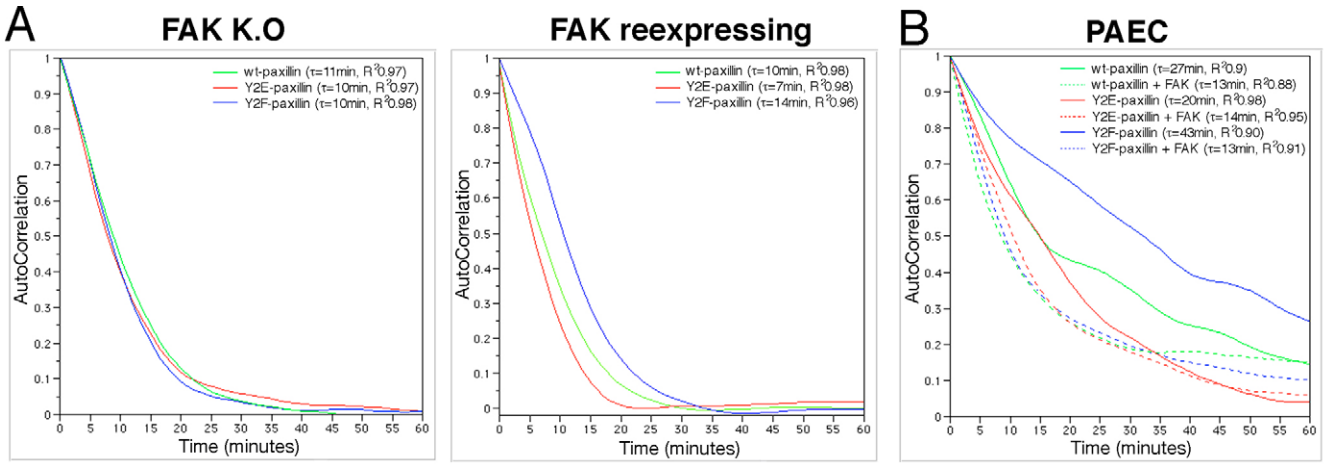

Fig. 8. FAK mediates the effect of paxillin phosphorylation on adhesion dynamics. Paxillin phosphorylation mutants do not have any effect on adhesion dynamics when expressed in FAK-knockout mouse embryonic fibroblasts (MEFs), whereas they do affect the dynamics in FAK-knockout cells re-expressing FAK (A). Displayed are smoothing spline fits (λ=100) based on autocorrelation analysis on nine movies for each condition. When FAK is expressed along with wild-type paxillin in PAECs, it substantially increases adhesion dynamics (B). Expression of Y2E-paxillin or Y2F-paxillin along with FAK does not modify the dynamics any further. The time constant for the correlation decay (τ) is given in parentheses, along with the R^2 of the fitting spline fit.

However, our data show that phosphorylation of paxillin at positions Y31 and/or Y118 substantially increases its affinity to FAK. Our biochemical analysis shows a fivefold increase in the binding of FAK to the phosphomimetic mutant of paxillin, compared with its binding to the non-phosphorylatable form. Moreover, quantification of immunostaining suggests a tenfold enrichment of FAK along structures containing the phosphomimetic paxillin, compared with its binding to structures dominated by the non-phosphorylatable molecule. It is not clear how the phosphorylation at positions Y31 and/or Y118 affect the interaction with FAK, yet it is conceivable that the phosphorylation induces a conformational change that makes the LD motifs more accessible to FAK.

The mechanism whereby FAK upregulates the turnover of integrin adhesions (Ilic et al., 1995; von Wichert et al., 2003; Webb et al., 2004) is still largely unclear. One possible explanation is that FAK activates calpains, which are known to cleave several FA proteins, including paxillin, vinculin and talin (Franco and Huttenlocher, 2005). Another possibility is that FAK might regulate actomyosin contractility by suppressing Rho activity (Ren et al., 2000). Irrespective of the mechanism underlying FAK action, we expect that low phosphopaxillin levels force FAK to disengage from the adhesion site, indirectly leading to increased adhesion stability.

Another interesting topic highlighted herein concerns the role of paxillin in FB formation. In the past, paxillin was not appreciated as a major component of FBs (Zamir et al., 1999), probably because its intensity in these adhesions is <30%, compared with its intensity in FAs. However, we demonstrate that not only is non-phosphorylated paxillin a component of FBs, but that paxillin dephosphorylation is obligatory for FB formation. Previous studies using GFP-tensin as a FB marker showed that these adhesions 'emerge' centripetally from FA, in an actomyosin-dependent manner (Zamir et al., 1999). Apparently, paxillin dephosphorylation unlocks FAs and enables FB development. As shown here, this process affects not only the cellular adhesion system, but has a long-range effect on the reorganization of the ECM fibrillogenesis.

Integration of the data presented here enables us to propose a comprehensive model addressing the interplay between paxillin phosphorylation, FAK, and mechanical forces, and their role in the assembly of integrin adhesions (Fig. 9A). These processes were further developed into a mathematical model (see Materials and Methods). This model was constructed as a set of three coupled ordinary differential equations, and a representative output of their solution is presented in Fig. 9B. The proposed model assumes that the assembly of FX is driven by the recruitment of phosphopaxillin (probably phosphorylated by Src) that serves as a docking site for FAK, which, in turn, induce disassembly of these short-lived adhesions. In this model, application of mechanical force induces paxillin dephosphorylation, which leads to dissociation of FAK from the complex and thus to the apparent stabilization of the adhesion and to its growth.

In Fig. 9C we summarize the functional relationships between FAK, phosphopaxillin and paxillin and the three forms of integrin-mediated adhesions. A negative feedback loop between FAK and phosphopaxillin underlies the assembly and turnover of FXs. Force-induced increase in non-

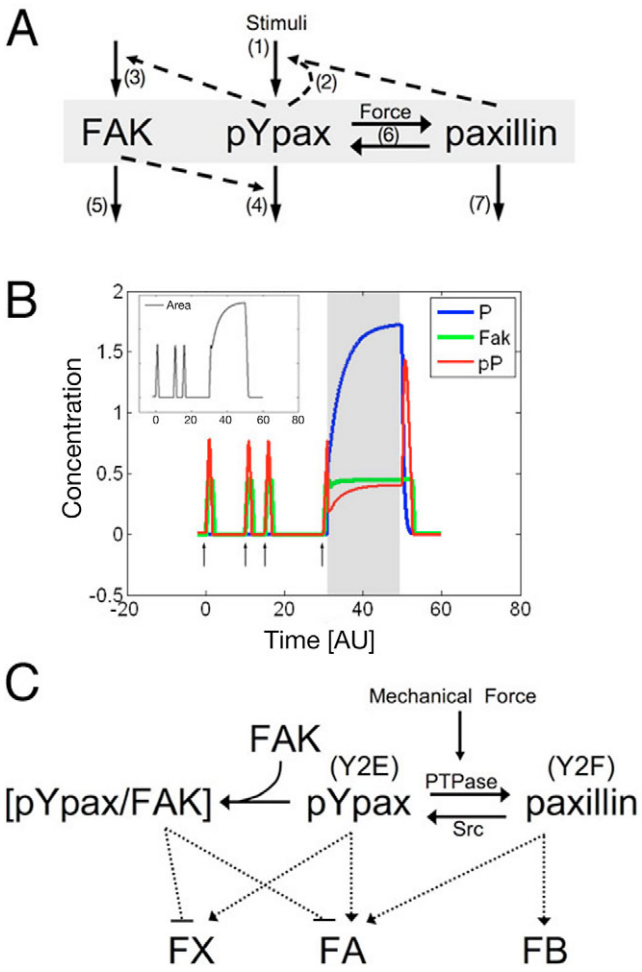

Fig. 9. Hypothetical model suggesting the involvement of a switch between phosphorylated and non-phosphorylated paxillin and a negative feedback loop with FAK in the regulation of adhesion dynamics. (A) Based on the results in this paper we constructed a working model composed of the following assumptions: (1) Phosphopaxillin is initially recruited following an external stimuli (integrin adhesion). (2) Thereafter its recruitment rate is positively regulated by the existence of both phosphopaxillin and paxillin. (3) FAK recruitment into the adhesion is dependent on phosphopaxillin concentration. (4) Phosphopaxillin disassembles in a FAK-dependent manner where FAK concentration increases the disassembly rate. (5) FAK disassembly occurs at the same rate it assembles, after a short delay. (6) Phosphopaxillin becomes dephosphorylated at a high rate when mechanical force exists and paxillin becomes phosphorylated constantly at a low rate. (7) Paxillin disassembles at a constant rate. (B) The above assumptions were compiled into a set of three simple differential equations (see model in Materials and Methods) and their solutions for the changing concentration of phosphopaxillin (red), FAK (green) and paxillin (blue) are given here in graphical form. Arrows under the time line mark the adhesion stimuli. Gray shading depicts the existence of mechanical force. The change over time in adhesion 'area' (sum of paxillin and phosphopaxillin) is presented in the insert. (C) This hypothetical scheme presents the manner by which a paxillin phosphorylation switch and FAK might regulate the formation of the three integrin-mediated adhesion forms: focal complexes (FX), focal adhesions (FA) and fibrillar adhesions (FB).

phosphorylated paxillin levels underlies the transformation of FXs into FAs. Paxillin phosphorylation and dephosphorylation can also dominate the dynamics of mature FAs. Thus, polarized distribution of phosphopaxillin may lead to FAs 'treadmilling' toward the cell center. Finally, the apparent dephosphorylation of paxillin, close to the edge of the FAs pointing toward the cell center, is a key event that enables FB formation and, as a consequence, ECM fibrillogenesis.

In summary, the proposed model accounts for many of the dynamic processes that have been observed in the different forms of integrin adhesions, and suggests a unifying mechanism for their regulated development. Though oversimplified, the model highlights a single element (i.e. the state of paxillin phosphorylation) as a key switch that regulated the fate of the adhesion site.

Materials and Methods

cDNAs and antibodies

YFP-paxillin was constructed by recloning the published GFP construct (Zamir et al., 2000) into the pEYFP vector (Clontech, Palo-Alto, CA). The paxillin phosphorylation mutants, in which both tyrosine 31 and 118 were replaced either by glutamic acid (phosphomimetic) or phenylalanine (non-phosphorylatable) were constructed by three consecutive PCR reactions, in which the PCR products of the first and second PCRs served as templates for the second and third reactions. (For a detailed description of primers and PCR conditions, see Tables S1 and S2 in supplementary material.) High-fidelity Psp DNA polymerase (Bioron, Ludwigshafen, Germany) was used for all PCR reactions, and the resulting sequences validated by direct sequencing. GFP-FAK was kindly provided by Kenneth M. Yamada (NIH, Bethesda, MD).

Primary antibodies used in this work were: Mouse anti-paxillin and mouse anti-FAK (BD Transduction Laboratories, Lexington, KY); rabbit anti-phosphorylated paxillin (Y118 or Y31) and rabbit anti-phosphorylated FAK (Y397) (Biosource, Camarillo, CA); mouse anti-PY 4G10 (Upstate Biotechnology, Charlottesville, VA). Rabbit anti-human tensin 1 was a gift of Su Hao Lo (University of California-Davis, Sacramento, CA); rabbit anti-human fibronectin was prepared in our lab by Tova Volberg, by injecting rabbits with human plasma fibronectin. Phosphospecific antibodies were tested by western blot against whole cell lysates, to verify their specificity. Secondary antibodies were: goat anti-mouse or anti-rabbit, conjugated to Cy3, Cy5 or Alexa Fluor 488 (Jackson ImmunoResearch Laboratories, West Grove, PA). Actin was labeled with phalloidin, conjugated to TRITC (Sigma Chemical Co., St Louis, MO).

Cell culture, transfection and immunostaining

Primary porcine aortic endothelial cells (kindly provided by Avrum Gotlieb, Toronto General Hospital, Toronto, Canada) were cultured in M199 medium with Earle's salts, L-glutamine and $NaHCO_3$ (Sigma) supplemented with 10% FCS (Biological Industries, Beit Haemek, Israel), at 37°C in a 5% CO_2 humidified atmosphere. FAK-deficient mouse embryo fibroblasts, cultured from E8.0 embryos, and FAK-deficient cells, re-expressing FAK cells, were kindly provided by Dusko Ilic (UCSF, San-Francisco, CA). Rat embryo fibroblast (REF52) lines stably expressing YFP-paxillin were prepared by Irena Lavelin and Yael Paran in our lab. Embryo fibroblasts were grown in DMEM medium supplemented with 10% FCS.

PAECs and the FAK-null cells were transfected in 24-well plates, using 2.5 μl Lipofectamine2000 (Invitrogen, Carlsbad, CA) with 2.5 μg of DNA. Four hours later, the cells were replated onto 13-mm round coverslips or glass-bottomed culture dishes (MaTek, Ashland, MA) pre-coated with fibronectin (5 μg/ml, Sigma). NIH3T3 cells were transfected with Lipofectamine Plus (Invitrogen) according to the manufacturer's instructions. For double transfections of FAK and the paxillin mutants, equal amounts of DNA from both constructs were used. Cells, processed for immunostaining, were fixed for 2 minutes in warm 3% paraformaldehyde (PFA) + 0.5% Triton X-100, and then post-fixed with PFA alone for an additional 40 minutes. After fixation, cells were washed in PBS and incubated with the primary and secondary antibodies in a humid chamber, for 1 hour each. After washing with PBS, cells were mounted in Elvanol (Mowiol 4-88, Hoechst, Frankfurt, Germany).

To inhibit cellular contractility cells were incubated with 100 μM 1-(5-iso-quinolinylsulfonyl)-2-methylpiperazine (H-7; I-7016; Sigma, St Louis, MO).

Image acquisition and live-cell imaging

Time-lapse movies as well as images of fixed cells were recorded using the Real Time (RT) DeltaVision System (Applied Precision, Issaquah, WA), consisting of an Olympus IX71 inverted microscope equipped with a CoolSnap HQ camera (Photometrics, Tucson, AZ) and weather station temperature controller, operated by SoftWoRx and Resolve3D software (Applied Precision). Images were acquired with an Olympus planApoN 60× /1.42 objective, with or without an additional 1.6× auxiliary magnification. For live cells, DMEM containing 25 mM HEPES, without Phenol Red and riboflavin (Biological Industries) and supplemented with 10% FCS was used, in order to maintain a pH of 7.04 throughout the experiments.

Image analysis and statistics

All image analysis was carried out using Priism software for Linux (http://msg.ucsf.edu/IVE/Download). Temporal and component ratio images were calculated and presented as previously described (Zamir et al., 1999). Autocorrelation analysis was performed on movies that were high-pass filtered, after determining a threshold above which all pixels were defined as parts of adhesion structures. To separately analyze FA and FB, polygons were manually drawn around the respective regions. A mask was created by all pixels above the threshold in the first frame. In each consecutive frame, the sum of intensities of all pixels within this mask was multiplied by the sum of intensities in the first frame. The resulting values were normalized, so that the multiplication of the first frame by itself would equal one. This measure of autocorrelation takes into account both a reduction in intensity of an adhesion, and misalignment resulting from movement of an adhesion. As both phenomena are indicative of disassembly, we view this autocorrelation index as an indicator of adhesion dynamics.

Measurement of the number of adhesions and their average intensity was performed by segmentation of the images with the "water" algorithm as previously described (Zamir et al., 1999).

Line profiles displaying the relative staining intensity of paxillin along a line one pixel wide, and average intensity measurements of fibronectin within cells marked by a polygon, were performed in Priism.

Data were regularly registered using Microsoft Excel X. Statistical analyses, including means and standard deviations, Student's *t*-test and smoothing spline fits and graphs, were carried out with JMP IN software, version 4.0.3 (SAS Institute, Cary, NC). Images were prepared for publication using Adobe Photoshop 7.0 (Adobe Systems, San Jose, CA).

Production of GST-Paxillin

Wild-type paxillin and the two mutants were excised from the YFP vector by PCR, and subcloned into the GST fusion vector pGEX-6P1 (GE HealthCare, Piscataway, NJ). Protein concentrations were determined by running samples on SDS-PAGE along with known concentrations of BSA, and visualizing the resulting bands using GelCode Blue stain reagent (Pierce, Rockford, IL). *E. coli* BL-21 transformed with pGEX-Paxillin were grown in 40 ml LB overnight at 37°C. The culture was then diluted into 400 ml LB and grown at 37°C until OD_{600} reached 0.6. Then, IPTG was added to a final concentration of 0.2 mM and the bacterial culture was grown for an additional period of 3 hours at 30°C. The bacteria were pelleted by centrifugation and then resuspended in 10 ml of 50 mM Tris-HCl, 150 mM NaCl, 1 mM EDTA, 1 mM DTT, and 10 μl/ml Protease inhibitor cocktail (P8465, Sigma-Aldrich), pH 8. The suspension was sonicated five times with 20-second pulses and pauses and then centrifuged at 4°C. The supernatant was transferred to a new tube and mixed with 1.6 ml of 50% glutathione Sepharose 4B beads, after they were washed twice with bacteria resuspension buffer. The beads and bacterial extract were incubated for 2 hours at 4°C (with agitation), after which the beads were washed twice with 50 mM Tris-HCl pH 8, 1 mM EDTA, 1 mM DTT and protease inhibitors, followed by two washes with 50 mM Tris-HCl pH 8, 1 mM EDTA, 1 mM DTT and 100 mM NaCl. After the last wash the beads, conjugated to GST-paxillin, were resuspended in 2 ml, divided into aliquots and frozen in liquid nitrogen.

Pull-down assay

Porcine aortic endothelial cells in confluent 15 cm plates were washed with cold PBS, and then lysed with buffer containing: 50 mM Tris-HCl, 1% NP-40, 120 mM NaCl, 2.5 mM EGTA, 1 mM NaF, 1 mM VO_3, 10 mM MgCl, 1 mM DTT, 100 μg/ml PMSF and 10 μl/ml protease inhibitor cocktail, pH 7.4. After centrifugation, the supernatant was incubated for 1 hour at 4°C (with agitation) with 50 μg of GST, conjugated to glutathione Sepharose beads, to reduce non-specific protein binding. After centrifugation, the pre-cleaned cell extract was incubated for 2 hours with 25 μg of either of the mutant paxillin GST fusion proteins, conjugated to glutathione Sepharose beads. Finally, the beads were washed three times with a wash buffer (50 mM Tris-HCl, 120 mM NaCl, 2.5 mM EGTA, 10 mM MgCl, pH 7.4) and boiled in 100 μl of 1× sample buffer. One-fifth of each pull-down was run on a 10% SDS gel, transferred to Hybond-C extra nitrocellulose (GE HealthCare), and blotted with anti-FAK antibodies. Bands were visualized using SuperSignal West Pico Chemiluminescent (Pierce), scanned by a Bio-Rad GS-700 imaging densitometer, and quantified using imageJ software.

Model for the regulation of focal adhesion dynamics by paxillin tyrosine phosphorylation

The model was constructed as a set of three coupled ordinary differential equations (ode). The equations were integrated using the built-in ode solver in the Matlab environment.

The equation for the rate of change of concentration of phosphopaxillin (pP) is:

$$d(pP)/dt = recruitmentInitiationSignal + b1*MM3*(t>0) - a1*MMdelay*(pP>0) - a4*stressSignal*pP + a5*P .$$

pP is recruited when there is an initiation of 'recruitment signal' (*recruitmentInitiationSignal*), such as a new integrin-ECM engagement. The recruitment signals used here are short pulses, with amplitude 1 and duration 0.1. Phosphorylated paxillin is recruited into the nascent adhesion only following the recruitment signal. We assume that pP recruitment is positively regulated by the levels of both *P* and *pP*. This is manifested by a regulation composed of a Michaelis-Menten (*MM*) term, where the sum of *pP* and *P* affects the recruitment rate in a form of an activator: *MM3* = 1/{1 + [*k2*/(*pP*+*P*)]^*n2*}. Here both *pP* and *P* serve as activators of the process of pP recruitment. We assume a characteristic affinity, *k2*=0.1 and cooperativity *n2*=3. The basal level of recruitment is assumed to be zero. pP disassembles in a FAK-dependent manner where FAK local concentration, in the adhesion site, increases the disassembly rate. *a1*=5 is the maximal possible rate of disassembly by saturating amounts of FAK. Also we assume that FAK works in a delay after pP recruitment. The level of disassembly is thus given by an MM term of the form: *MMdelay* = 1/[1 + (*k1*/*FDelay*)^*n1*], where FDelay is the concentration of FAK at an earlier time (delay=0.5). In this expression FAK serves as an activator of the disassembly process. *k1*=0.5 is the affinity, and *n1*=3 is the cooperativity. pP becomes dephosphorylated at a rate *a4*=10 following activation of mechanical stress (*stressSignal*=1) otherwise, *stressSignal*=0 and there is no dephosphorylation. P becomes phosphorylated at a rate *a5*=2.

The equation for the rate of change of concentration of Paxillin (P) is:

$$dP/dt = a4*stressSignal*pP - a5*P - a6*P .$$

Paxillin dissociates from the adhesion site at a constant rate *a6*=0.35, leading to its disassembly.

The equation for the rate of change of concentration of FAK (F) is:

$$dF/dt=b3*MM2 - b3*MM2delay*(F>0) .$$

FAK is recruited into the adhesion under the influence of *pP*. It is modeled as an MM term of the form: *MM2* = 1/[1 + (*k2*/*pP*)^*n2*]; where *pP* is an activator of the recruitment step. *b3*=1 is the maximal amplitude of recruitment, *k2*=0.1 is the affinity and *n2*=3 is the cooperativity. Rate of disassembly of FAK is equal to the rate of assembly but with a delay=0.5.

This study was supported by grants from the Israel Science Foundation and the National Institute of General Medical Sciences (NIGMS), National Institutes of Health Cell Migration Consortium, Grant U54 GM64346. Benjamin Geiger holds the Erwin Neter Professorial Chair in Cell and Tumor Immunology. Zvi Kam is the Israel Pollak Professor of Biophysics.

References

Ballestrem, C., Hinz, B., Imhof, B. A. and Wehrle-Haller, B. (2001). Marching at the front and dragging behind: differential alphaVbeta3-integrin turnover regulates focal adhesion behavior. *J. Cell Biol.* **155**, 1319-1332.

Barry, S. T. and Critchley, D. R. (1994). The RhoA-dependent assembly of focal adhesions in Swiss 3T3 cells is associated with increased tyrosine phosphorylation and the recruitment of both pp125FAK and protein kinase C-delta to focal adhesions. *J. Cell Sci.* **107**, 2033-2045.

Bellis, S. L., Perrotta, J. A., Curtis, M. S. and Turner, C. E. (1997). Adhesion of fibroblasts to fibronectin stimulates both serine and tyrosine phosphorylation of paxillin. *Biochem. J.* **325**, 375-381.

Bershadsky, A. D., Balaban, N. Q. and Geiger, B. (2003). Adhesion-dependent cell mechanosensitivity. *Annu. Rev. Cell Dev. Biol.* **19**, 677-695.

Bockholt, S. M. and Burridge, K. (1993). Cell spreading on extracellular matrix proteins induces tyrosine phosphorylation of tensin. *J. Biol. Chem.* **268**, 14565-14567.

Brown, M. C. and Turner, C. E. (2004). Paxillin: adapting to change. *Physiol. Rev.* **84**, 1315-1339.

Brown, M. C., Perrotta, J. A. and Turner, C. E. (1998). Serine and threonine phosphorylation of the paxillin LIM domains regulates paxillin focal adhesion localization and cell adhesion to fibronectin. *Mol. Biol. Cell* **9**, 1803-1816.

Burridge, K., Turner, C. E. and Romer, L. H. (1992). Tyrosine phosphorylation of paxillin and pp125FAK accompanies cell adhesion to extracellular matrix: a role in cytoskeletal assembly. *J. Cell Biol.* **119**, 893-903.

Cai, X., Li, M., Vrana, J. and Schaller, M. D. (2006). Glycogen synthase kinase 3- and extracellular signal-regulated kinase-dependent phosphorylation of paxillin regulates cytoskeletal rearrangement. *Mol. Cell. Biol.* **26**, 2857-2868.

Chrzanowska-Wodnicka, M. and Burridge, K. (1994). Tyrosine phosphorylation is involved in reorganization of the actin cytoskeleton in response to serum or LPA stimulation. *J. Cell Sci.* **107**, 3643-3654.

Critchley, D. R. (2000). Focal adhesions – the cytoskeletal connection. *Curr. Opin. Cell Biol.* **12**, 133-139.

Frame, M. C. (2004). Newest findings on the oldest oncogene; how activated src does it. *J. Cell Sci.* **117**, 989-998.

Franco, S. J. and Huttenlocher, A. (2005). Regulating cell migration: calpains make the cut. *J. Cell Sci.* **118**, 3829-3838.

Geiger, B., Bershadsky, A., Pankov, R. and Yamada, K. M. (2001). Transmembrane crosstalk between the extracellular matrix–cytoskeleton crosstalk. *Nat. Rev. Mol. Cell Biol.* **2**, 793-805.

Glenney, J. R., Jr and Zokas, L. (1989). Novel tyrosine kinase substrates from Rous sarcoma virus-transformed cells are present in the membrane skeleton. *J. Cell Biol.* **108**, 2401-2408.

Hamadi, A., Bouali, M., Dontenwill, M., Stoeckel, H., Takeda, K. and Ronde, P. (2005). Regulation of focal adhesion dynamics and disassembly by phosphorylation of FAK at tyrosine 397. *J. Cell Sci.* **118**, 4415-4425.

Hayashi, I., Vuori, K. and Liddington, R. C. (2002). The focal adhesion targeting (FAT) region of focal adhesion kinase is a four-helix bundle that binds paxillin. *Nat. Struct. Biol.* **9**, 101-106.

Ilic, D., Furuta, Y., Kanazawa, S., Takeda, N., Sobue, K., Nakatsuji, N., Nomura, S., Fujimoto, J., Okada, M. and Yamamoto, T. (1995). Reduced cell motility and enhanced focal adhesion contact formation in cells from FAK-deficient mice. *Nature* **377**, 539-544.

Iwasaki, T., Nakata, A., Mukai, M., Shinkai, K., Yano, H., Sabe, H., Schaefer, E., Tatsuta, M., Tsujimura, T., Terada, N. et al. (2002). Involvement of phosphorylation of Tyr-31 and Tyr-118 of paxillin in MM1 cancer cell migration. *Int. J. Cancer* **97**, 330-335.

Kassenbrock, C. K. and Anderson, S. M. (2004). Regulation of ubiquitin protein ligase activity in c-Cbl by phosphorylation-induced conformational change and constitutive activation by tyrosine to glutamate point mutations. *J. Biol. Chem.* **279**, 28017-28027.

Kaverina, I., Krylyshkina, O. and Small, J. V. (2002). Regulation of substrate adhesion dynamics during cell motility. *Int. J. Biochem. Cell Biol.* **34**, 746-761.

Kiyokawa, E., Hashimoto, Y., Kobayashi, S., Sugimura, H., Kurata, T. and Matsuda, M. (1998a). Activation of Rac1 by a Crk SH3-binding protein, DOCK180. *Genes Dev.* **12**, 3331-3336.

Kiyokawa, E., Hashimoto, Y., Kurata, T., Sugimura, H. and Matsuda, M. (1998b). Evidence that DOCK180 up-regulates signals from the CrkII-p130(Cas) complex. *J. Biol. Chem.* **273**, 24479-24484.

Nakamura, K., Yano, H., Uchida, H., Hashimoto, S., Schaefer, E. and Sabe, H. (2000). Tyrosine phosphorylation of paxillin alpha is involved in temporospatial regulation of paxillin-containing focal adhesion formation and F-actin organization in motile cells. *J. Biol. Chem.* **275**, 27155-27164.

Nayal, A., Webb, D. J., Brown, C. M., Schaefer, E. M., Vicente-Manzanares, M. and Horwitz, A. R. (2006). Paxillin phosphorylation at Ser273 localizes a GIT1-PIX-PAK complex and regulates adhesion and protrusion dynamics. *J. Cell Biol.* **173**, 587-589.

Nobes, C. D. and Hall, A. (1995). Rho, rac, and cdc42 GTPases regulate the assembly of multimolecular focal complexes associated with actin stress fibers, lamellipodia, and filopodia. *Cell* **81**, 53-62.

Panetti, T. S. (2002). Tyrosine phosphorylation of paxillin, FAK, and p130CAS: effects on cell spreading and migration. *Front. Biosci.* **7**, d143-d150.

Pankov, R., Cukierman, E., Katz, B. Z., Matsumoto, K., Lin, D. C., Lin, S., Hahn, C. and Yamada, K. M. (2000). Integrin dynamics and matrix assembly: tensin-dependent translocation of alpha(5)beta(1) integrins promotes early fibronectin fibrillogenesis. *J. Cell Biol.* **148**, 1075-1090.

Petit, V., Boyer, B., Lentz, D., Turner, C. E., Thiery, J. P. and Valles, A. M. (2000). Phosphorylation of tyrosine residues 31 and 118 on paxillin regulates cell migration through an association with CRK in NBT-II cells. *J. Cell Biol.* **148**, 957-970.

Potter, M. D., Barbero, S. and Cheresh, D. A. (2005). Tyrosine phosphorylation of VE-cadherin prevents binding of p120- and beta-catenin and maintains the cellular mesenchymal state. *J. Biol. Chem.* **280**, 31906-31912.

Ren, X. D., Kiosses, W. B., Sieg, D. J., Otey, C. A., Schlaepfer, D. D. and Schwartz, M. A. (2000). Focal adhesion kinase suppresses Rho activity to promote focal adhesion turnover. *J. Cell Sci.* **113**, 3673-3678.

Retta, S. F., Barry, S. T., Critchley, D. R., Defilippi, P., Silengo, L. and Tarone, G. (1996). Focal adhesion and stress fiber formation is regulated by tyrosine phosphatase activity. *Exp. Cell Res.* **229**, 307-317.

Richardson, A., Malik, R. K., Hildebrand, J. D. and Parsons, J. T. (1997). Inhibition of cell spreading by expression of the C-terminal domain of focal adhesion kinase (FAK) is rescued by coexpression of Src or catalytically inactive FAK: a role for paxillin tyrosine phosphorylation. *Mol. Cell. Biol.* **17**, 6906-6914.

Ridley, A. J. and Hall, A. (1994). Signal transduction pathways regulating Rho-mediated stress fibre formation: requirement for a tyrosine kinase. *EMBO J.* **13**, 2600-2610.

Rottner, K., Hall, A. and Small, J. V. (1999). Interplay between Rac and Rho in the control of substrate contact dynamics. *Curr. Biol.* **9**, 640-648.

Schaller, M. D. and Parsons, J. T. (1995). pp125FAK-dependent tyrosine phosphorylation of paxillin creates a high-affinity binding site for Crk. *Mol. Cell. Biol.* **15**, 2635-2645.

Schaller, M. D. and Schaefer, E. M. (2001). Multiple stimuli induce tyrosine phosphorylation of the Crk-binding sites of paxillin. *Biochem. J.* **360**, 57-66.

Schlaepfer, D. D. and Mitra, S. K. (2004). Multiple connections link FAK to cell motility and invasion. *Curr. Opin. Genet. Dev.* **14**, 92-101.

Tachibana, K., Sato, T., D'Avirro, N. and Morimoto, C. (1995). Direct association of pp125FAK with paxillin, the focal adhesion-targeting mechanism of pp125FAK. *J. Exp. Med.* **182**, 1089-1099.

Tomar, A., Wang, Y., Kumar, N., George, S., Ceacareanu, B., Hassid, A., Chapman, K. E., Aryal, A. M., Waters, C. M. and Khurana, S. (2004). Regulation of cell motility by tyrosine phosphorylated villin. *Mol. Biol. Cell* **15**, 4807-4817.

Tsubouchi, A., Sakakura, J., Yagi, R., Mazaki, Y., Schaefer, E., Yano, H. and Sabe,

H. (2002). Localized suppression of RhoA activity by Tyr31/118-phosphorylated paxillin in cell adhesion and migration. *J. Cell Biol.* **159**, 673-683.

Turner, C. E., Pietras, K. M., Taylor, D. S. and Molloy, C. J. (1995). Angiotensin II stimulation of rapid paxillin tyrosine phosphorylation correlates with the formation of focal adhesions in rat aortic smooth muscle cells. *J. Cell Sci.* **108**, 333-342.

Volberg, T., Romer, L., Zamir, E. and Geiger, B. (2001). pp60(c-src) and related tyrosine kinases: a role in the assembly and reorganization of matrix adhesions. *J. Cell Sci.* **114**, 2279-2289.

von Wichert, G., Haimovich, B., Feng, G. S. and Sheetz, M. P. (2003). Force-dependent integrin-cytoskeleton linkage formation requires downregulation of focal complex dynamics by Shp2. *EMBO J.* **22**, 5023-5035.

Webb, D. J., Donais, K., Whitmore, L. A., Thomas, S. M., Turner, C. E., Parsons, J. T. and Horwitz, A. F. (2004). FAK-Src signalling through paxillin, ERK and MLCK regulates adhesion disassembly. *Nat. Cell Biol.* **6**, 154-161.

Wierzbicka-Patynowski, I. and Schwarzbauer, J. E. (2003). The ins and outs of fibronectin matrix assembly. *J. Cell Sci.* **116**, 3269-3276.

Yano, H., Uchida, H., Iwasaki, T., Mukai, M., Akedo, H., Nakamura, K., Hashimoto, S. and Sabe, H. (2000). Paxillin alpha and Crk-associated substrate exert opposing effects on cell migration and contact inhibition of growth through tyrosine phosphorylation. *Proc. Natl. Acad. Sci. USA* **97**, 9076-9081.

Zaidel-Bar, R., Ballestrem, C., Kam, Z. and Geiger, B. (2003). Early molecular events in the assembly of matrix adhesions at the leading edge of migrating cells. *J. Cell Sci.* **116**, 4605-4613.

Zaidel-Bar, R., Kam, Z. and Geiger, B. (2005). Polarized downregulation of the paxillin-p130CAS-Rac1 pathway induced by shear flow. *J. Cell Sci.* **118**, 3997-4007.

Zamir, E. and Geiger, B. (2001). Molecular complexity and dynamics of cell-matrix adhesions. *J. Cell Sci.* **114**, 3583-3590.

Zamir, E., Katz, B. Z., Aota, S., Yamada, K. M., Geiger, B. and Kam, Z. (1999). Molecular diversity of cell-matrix adhesions. *J. Cell Sci.* **112**, 1655-1669.

Zamir, E., Katz, M., Posen, Y., Erez, N., Yamada, K. M., Katz, B. Z., Lin, S., Lin, D. C., Bershadsky, A., Kam, Z. et al. (2000). Dynamics and segregation of cell-matrix adhesions in cultured fibroblasts. *Nat. Cell Biol.* **2**, 191-196.